

Dalton Transactions

An international journal of inorganic chemistry

rsc.li/dalton



ISSN 1477-9226



Cite this: *Dalton Trans.*, 2024, **53**, 2929

Received 21st October 2023,
Accepted 30th November 2023
DOI: 10.1039/d3dt03509c
rsc.li/dalton

Diphosphene with a phosphineborane tether and its rhodium complex[†]

Akihiro Tsurusaki, Shingo Takechi and Ken Kamikawa *

A diphosphene ligand possessing a $P=P$ bond and a phosphineborane moiety in its molecule was synthesized. The reaction of the new bidentate diphosphene–phosphineborane ligand with $[Rh(cod)_2]BF_4$ provided a cationic diphosphene–rhodium complex with *cis*-coordination through the η^1 - $P=P$ and η^2 - BH_3 moieties. The complex was applied to the coupling reaction of benzimidazole with cyclohexylallene. The complex also underwent a ligand exchange reaction with N-donor reagents such as *N*-methylpyrrolidine and *N,N,N,N*-tetramethylethylenediamine. In particular, the addition reaction of pyridine with the rhodium complex provided an equilibrium mixture of the rhodium complex, pyridine, the diphosphene–phosphineborane ligand, and $[Rh(pyridine)_2(cod)]BF_4$.

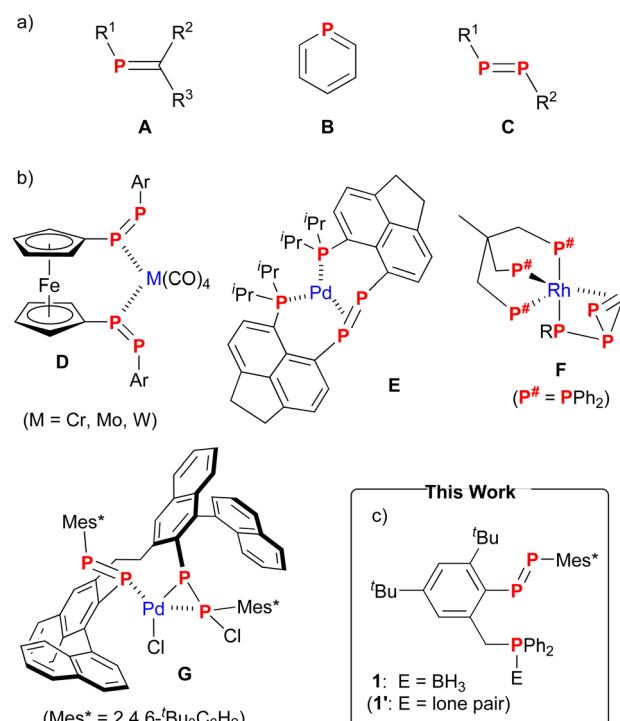
Introduction

Organophosphorus compounds are one of the most common organic ligands for transition metals, yielding molecules with diverse structures in organometallic chemistry.¹ A variety of sterically and electronically tuned trivalent phosphorus compounds act as σ -donor ligands through their lone pairs.^{1c,d} On the other hand, low-coordinate phosphorus compounds, such as phosphaalkenes **A** and phosphinines **B**, are strong π -acceptors owing to the low-lying π^* orbital of the $P=C$ bonds (Fig. 1a).² Some transition metal complexes are utilized in transition-metal-catalyzed organic transformations.^{1c,2c-f,3,4}

Diphosphenes **C** with a $P=P$ bond in the molecules are also low-coordinate phosphorus compounds that captivated chemists early on.^{5,6} The LUMO level of the $P=P$ π^* orbital in diphosphenes is lower than that of the $P=C$ π^* orbital in phosphaalkenes or phosphinines,⁷ which should enhance the π -accepting character of the transition metals. We recently demonstrated that a gold complex of diphosphene with a 1,1'-binaphthyl group is an active catalyst for the intramolecular hydroarylation of aryl alkynyl ethers.⁸ In contrast, monodentate diphosphenes hardly form stable complexes with late transition metals including rhodium(I) and palladium(II), which are known to promote a wide variety of catalytic organic transformations. One solution for generating robust complexes is to increase the coordination ability of diphosphenes by using a

multidentate ligand. The combination of a $P=P$ bond and other coordinating moieties (e.g., phosphine and amine) holds promise for creating new coordination environments.

Multidentate diphosphene–transition metal complexes are in their infancy compared with their monodentate counter-



Department of Chemistry, Graduate School of Science, Osaka Metropolitan University, 1-1 Gakuen-cho, Naka-ku, Sakai, Osaka 599-8531, Japan.
E-mail: tsurusaki@omu.ac.jp, kamikawa@omu.ac.jp

† Electronic supplementary information (ESI) available. CCDC 2301466 and 2301467. For ESI and crystallographic data in CIF or other electronic format see DOI: <https://doi.org/10.1039/d3dt03509c>

Fig. 1 (a) Phosphaalkenes **A**, phosphinines **B**, and diphosphenes **C**. (b) Complexes **D–G** with a multidentate ligand including $P=P$ bonds. (c) Diphosphene–phosphineborane ligand **1** (this work).

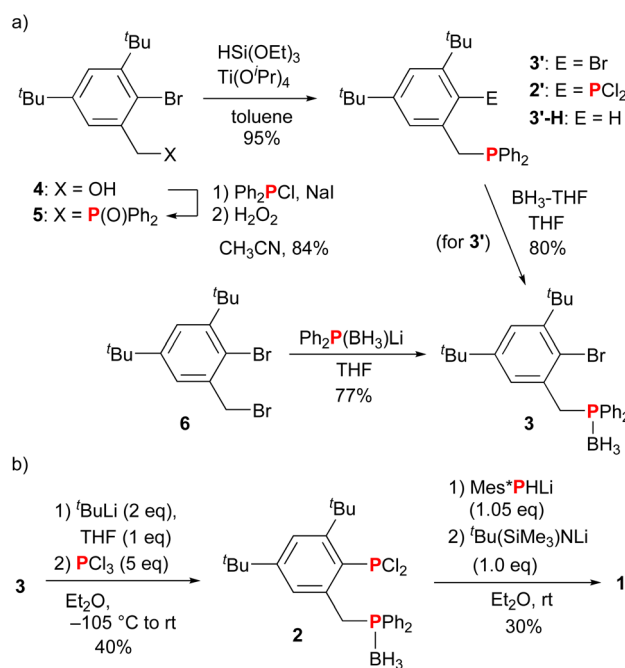


parts that appeared in the 1970s.^{9,10} Examples of diphosphene complexes with a multidentate ligand include Group 6 carbonyl complexes of bis(diphosphenyl)ferrocene **D**¹¹ and Group 10 complexes with a P=P bond and two phosphines^{12,13} (e.g., **E**¹²) (Fig. 1b). Complexes **D** are synthesized from bis(diphosphene) by a ligand exchange reaction,¹¹ whereas the P=P bond in Group 10 complexes is formed by the dimerization of a masked phosphinidene^{12,13} (phosphanylidene–phosphorane for **E**¹²). Rhodium complexes **F** with a P₄R moiety (R = H, alkyl) are obtained by the reaction of a trihydride- (L₃RhH₃) or an alkyl(ethylene)rhodium (L₃RhR(C₂H₄)) complex with P₄.¹⁴ The P₄R moiety in **F** acts as a bidentate ligand with an η^2 -coordinated P=P bond in the P₃ ring and a phosphido (PR) group. Our recently reported η^1 -diphosphene/ η^2 -phosphanylphosphido palladium complex **G** is derived from bis(diphosphene) via chloride migration from palladium to phosphorus.¹⁵ To create a diverse array of diphosphene–transition metal complexes with different coordination environments, unsymmetrical bidentate ligands bearing a P=P bond are of paramount importance. Such ligands should contribute to expanding the organometallic chemistry of diphosphenes through a direct ligand exchange reaction with a suitable precursor of transition metal complexes. To the best of our knowledge, there are no examples of stable diphosphenes with an additional coordinating moiety, the reason primarily being the inherent synthetic challenges in forging the highly reactive P=P bond. This situation sharply contrasts the abundance of multidentate ligands in phosphaalkenes and phosphinines in combination with oxazoline, pyridine, phosphine, etc.^{16,17} In this regard, we planned to synthesize diphosphene **1** with a P=P bond and a phosphine (Fig. 1c). A phosphinomethyl group was selected as a tether to a benzene ring on the basis of previous reports on bisphosphine ligands with a 2-methylbenzen-diyli (–C₆H₄CH₂–) linker¹⁸ and the facile synthesis of bulky aryl groups¹⁹ to protect the reactive P=P bond. Although we were unable to obtain **1**' despite numerous attempts, we were able to synthesize diphosphene **1** with a phosphineborane moiety. Newly obtained diphosphene–phosphineborane ligand **1** was used in the complexation with rhodium, and the results are described herein.

Results and discussion

Synthesis of diphosphene–phosphineborane ligand **1**

At the initial stage, we attempted to synthesize dichlorophosphine derivative **2**' from bromo derivative **3**' with a diphenylphosphinomethyl tether (Scheme 1). Compound **3**' was synthesized in two steps from 2-bromo-3,5-di-*tert*-butyl-1-(hydroxymethyl)benzene (**4**): the Michaelis–Arbuzov reaction of **4** employing Wang's conditions²⁰ gave phosphine oxide **5** in 84% yield, and then **5** was reduced by triethoxsilane and titanium(IV) tetraisopropoxide to give **3**' in 95% yield (Scheme 1a). When **3**' was reacted with ¹BuLi in THF at –78 °C and then PCl₃ was added, the protonated product **3**'-H, in which bromine in **3**' was replaced with hydrogen, was obtained in an



Scheme 1 (a) Synthesis of phosphine **3**' and phosphineborane **3**. (b) Synthesis of diphosphene–phosphineborane ligand **1**.

almost quantitative yield (data not shown). Changing the reaction conditions such as solvent (Et₂O and toluene) and temperature was insufficient to overcome the situation. This result was in sharp contrast to the synthesis of di-*tert*-butylphenyldichlorophosphines with dialkylamino, aryloxy, and methoxy groups at the methyl tether.¹⁹ Müller *et al.* revealed the molecular structure of (*o*-lithiobenzyl)dimethylphosphine, in which the phosphine moiety is coordinated to lithium.²¹ From this, we speculated that related lithium species with the coordination of phosphorus atom would prevent access by phosphorus reagent (PCl₃). Next, we turned our attention to borane-protected phosphine derivative **3**'.²² Compound **3** was obtained in 80% yield by the reaction of **3**' with borane–tetrahydrofuran complex. Alternatively, it was directly obtained by the reaction of 2-bromo-1-bromomethyl-3,5-di-*tert*-butylbenzene (**6**) with a borane-protected lithium phosphido, Ph₂P(BH₃)Li, in 77% yield. After the optimization of the reaction conditions, we isolated dichlorophosphine **2** in 40% yield by the lithium/bromine exchange reaction with ¹BuLi in Et₂O in the presence of 1 equiv. of THF at –105 °C and the addition of PCl₃ (Scheme 1b). We noted that a small amount of THF was required for the lithium/bromine exchange reaction. These reaction conditions were applied to the synthesis of **2**' without borane protection from phosphine **3**', but an unidentified mixture was generated without the formation of **2**'. Attempts to eliminate borane (BH₃) in **2** to give **2**' were also unsuccessful by the reaction with several amines,²³ such as *N*-methylpyrrolidine and 1,4-diazabicyclo[2.2.2]octane (DABCO), or trimethylphosphine in neat or toluene solution, giving a complex mixture. Next, the P=P bond was formed by



following a previously reported conventional method:^{5a} treatment of **2** with Mes*PHLi to form a P–P single bond and dehydrochlorination with ³Bu(SiMe₃)NLI as a base gave diphosphene–phosphineborane ligand **1** in 30% yield as a yellow solid. This result indicated that phosphineborane remained intact under the reaction conditions. The elimination of borane (BH₃) of **1** to obtain diphosphene–phosphine derivative **1'** was unsuccessful again: there was either no reaction or the formation of a complex mixture in the reaction of **1** with *N*-methylpyrrolidine or DABCO. The ³¹P NMR signals assignable to the P=P bond in **1** were observed at 531.3 and 483.1 ppm (¹J_{PP} = 578 Hz), which were comparable to those of unsymmetrically substituted diphosphenes with a Mes* group (e.g., Mes*P=PMes:^{24a} δ_P = 540.4, 467.6, ¹J_{PP} = 574 Hz; and Mes*P=PBNP:^{24b} δ_P = 458.7, 528.2, ¹J_{PP} = 569 Hz; BNp = 3-methyl-1,1'-binaphthylene-2-yl). The ³¹P and ¹¹B signals of the phosphineborane moiety at 22.1 and –37.1 ppm, respectively, were slightly shifted from those of **2** (δ_P = 20.7, δ_B = –38.2).

X-ray crystallographic analysis of **1** (Fig. 2a) showed that the P2 atom of the P=P bond and the P3 atom of the phosphinomethyl group are in a *trans* relationship with respect to central benzene **R**. The BH₃ group and the *tert*-butyl group at the *para* position of benzene **R** are oriented in the same direction. The P–P bond length (2.0406(8) Å) and the P–P–C bond angles (98.73(5)° and 100.39(6)°) are comparable to those of Mes*-substituted diphosphenes (Table S2†). The P–B bond length (1.924(2) Å) is also comparable to the (PhMe₂C)Ph₂P–BH₃ bond length (1.935(2) Å).²⁵ The IR spectrum of **1** exhibited moderately strong absorptions at 2400 and 2338 cm^{–1} owing to B–H stretching vibrations (Fig. S25†). The UV-vis spectrum measured in CH₂Cl₂ solution showed absorptions at 464 nm (ε, 400) and 338 nm (4190) as a shoulder (Fig. 3a), which were assigned to the n_π–π* and π–π* transitions of the P=P bond, respectively.^{5a,26}

Complexation of **1** with rhodium

Diphosphene–phosphineborane ligand **1** was directly used for complexation because rhodium complexes with a bidentate phosphine–phosphineborane ligand are known (Scheme 2).²⁷

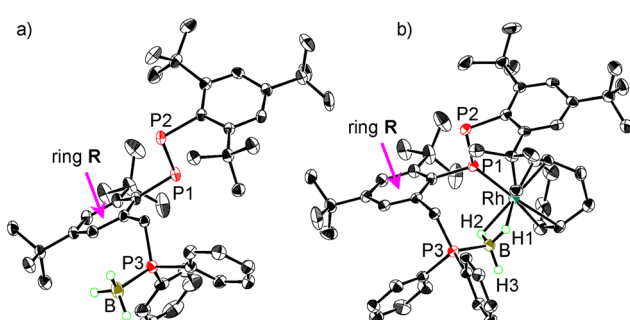


Fig. 2 Molecular structures of (a) diphosphene–phosphineborane ligand **1** and (b) diphosphene–rhodium complex **7**. Thermal ellipsoids are drawn at 50% probability. Hydrogen atoms except BH₃, anion BF₄[–], and solvated dichloroethanes in **7** are omitted for clarity.

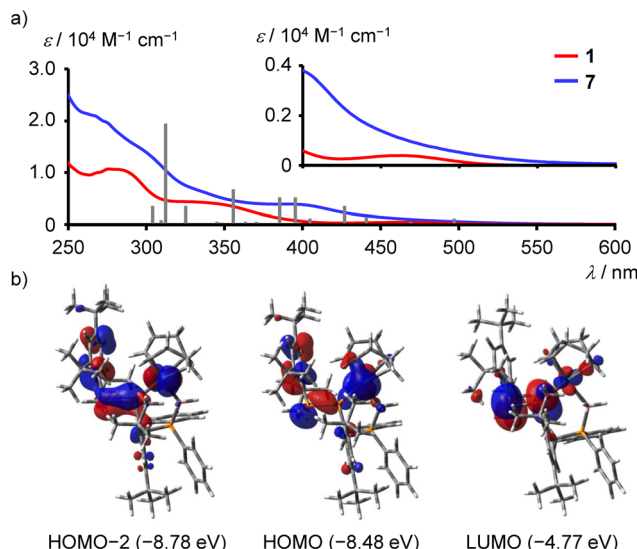
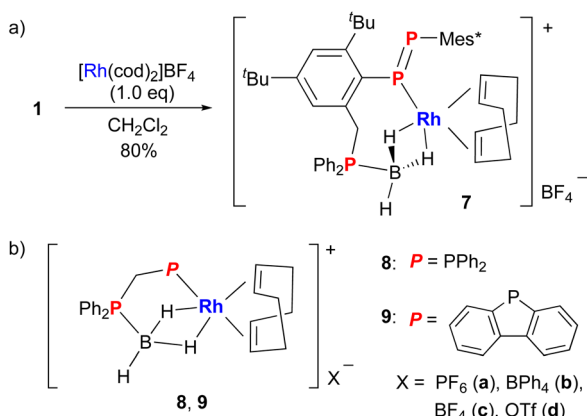


Fig. 3 (a) UV-vis absorption spectra of **1** (red) and **7** (blue) in CH₂Cl₂ solution. Gray bars represent calculated oscillator strengths of **7** longer than 300 nm. (b) Selected molecular orbitals of **7** (Isovalue = 0.03).



Scheme 2 (a) Synthesis of diphosphene–rhodium complex **7**. (b) Rhodium complexes **8** and **9** with a phosphine–phosphineborane ligand.

Treatment of **1** with 1 equiv. of [Rh(cod)₂]BF₄ in CH₂Cl₂ afforded diphosphene–rhodium complex **7** in 80% yield as a red-orange solid (Scheme 2a). This is the first example of a diphosphene–rhodium complex directly synthesized from a stable diphosphene. In contrast, treatment of **1** with 1 equiv. of [Ir(cod)₂]BF₄ in CD₂Cl₂ resulted in a complex mixture as judged from the ¹H and ³¹P NMR spectra of the crude mixture. The ³¹P NMR signals of **7** were observed at 439.8, 348.7, and 4.6 ppm. The two former chemical shifts and their coupling constant (¹J_{PP} = 544 Hz) supported the η¹-coordination of the P=P bond to a rhodium atom.^{5a,8} In addition, the signal at 348.7 ppm indicated the additional coupling to rhodium (¹J_{PRh} = 149 Hz). This value was larger than that of the η²-P=P bond of complex **F** (¹J_{PRh} = ca. 20 Hz)^{14a} owing to the coordination of the lone pair of phosphorus atom with high s contribution,

and was comparable to those of phosphine-rhodium complexes **8a** (145 Hz)^{27a} and **9b** (140 Hz).^{27b} The ³¹P signal of phosphineborane in **7** (4.6 ppm) was shifted upfield relative to that of **1** (22.1 ppm), whereas the ¹¹B chemical shift (−36.6 ppm) was comparable to that of **1** (−34.8 ppm). The coordination behavior of the BH_3 moiety was similar to that of **8a** and **9b**.²⁷ The BH_3 signal in the ¹H NMR spectrum was observed at −0.60 ppm as a broad doublet ($J = 105$ Hz) with the integral of three protons (Fig. S36†). This result indicated that the BH_3 group is fluxional in solution *via* a P–B bond rotation at room temperature. When a CD_2Cl_2 solution of **7** was cooled to −70 °C, the signal broadened, indicating coalescence. The peak observed at −0.60 ppm shifted to −1.47 ppm at −80 °C and then split into two independent signals −1.12 and −1.91 ppm upon further cooling to −90 °C. The two protons coordinated to rhodium at low temperatures under the non-equivalent environment. The third proton of BH_3 , which was observed around 2.4 ppm, could not be detected owing to the overlap to the CH_2 signal of cod. The IR spectrum of **1** exhibited weak absorptions at 2432, 2075, and 2008 cm^{-1} (Fig. S25†). The former frequency was due to the remaining B–H bond, whereas the latter two frequencies were due to the Rh–H bond in the solid state. The Rh–H vibration of $\text{HRh}(\text{CO})_2(\text{PPh}_3)_2$ was reported as 2038 cm^{-1} .²⁸ Theoretical calculations of the cation moiety of **7** at M06/SDD (Rh) and 6-31G(d) (other atoms) level of theory supported the B–H stretching (2449 cm^{-1}), the Rh–H antisymmetric stretching (2233 cm^{-1}), and the Rh–H symmetric stretching (2166 cm^{-1}) vibrations, where the values were scaled by 0.9585.²⁹ Although these calculated values deviated somewhat from the experimental ones, other vibrations were not estimated in the range of 2900 to 2000 cm^{-1} .

Recrystallization of **7** from a 1,2-dichloroethane/diisopropyl ether solution at −25 °C gave single crystals suitable for X-ray

crystallographic analysis (Fig. 2b). Hydrogen atoms on BH_3 were directly located in the difference Fourier map and refined isotropically. In the same manner as **1**, the P2 atom of the P=P bond and the P3 atom of the diphenylphosphinomethyl group are in a *trans* relationship with respect to central benzene R. One molecule each of diphosphene–phosphineborane ligand **1** and cod coordinates to rhodium, and **1** achieves *cis*-coordination through a phosphorus atom (P1) of diphosphene in an η^1 fashion and the BH_3 moiety in an η^2 fashion. The two B–H–Rh three-center two-electron bonds in **7** are similar to those in **8c**^{27a} and **9c**.^{27b} The P1–Rh–B angle (92.97 (9)°) in **7** is larger than that in **8c** (87.26(8)°) or **9c** (87.35(4)°) owing to the different carbon linkers (three carbon atoms in **7** *versus* one carbon atom in **8** and **9**). The P=P bond length of **7** (2.0413(13) Å) is comparable to the bond length of free ligand **1** (2.0406(8) Å), retaining the P=P double-bond character, and is slightly longer than those of η^1 -diphosphene Group 11 complexes (1.975(5)–2.0269(16) Å).^{8,30} The Rh–P1 bond length of **7** (2.2694(8) Å) lies between that of **8c** (2.2743(7) Å) and that of **9c** (2.2483(4) Å) (Table 1). To evaluate the effect of the nature of the coordinated phosphorus atom (P=PAR *vs.* PPh₂) and the length of the linker (methylene *vs.* 2-methylbenzen-diyl), theoretical calculations were carried out at M06/SDD (Rh) and 6-31G(d) (other atoms) level of theory for the cation moieties of complexes **7** and **8c** together with **7'** with hydrogen atoms instead of five *tert*-butyl groups in **7**; **10** with the P=PPh group and a methylene linker; and **11** with the PPh₂ group and a 2-methylbenzen-diyl linker (Table 1). The Rh–P1 bonds in the diphosphene complexes with a P=PPh moiety (2.294 Å in **7'** and 2.310 Å in **10**) are shorter than those in the phosphine complexes (2.390 Å in **11** and 2.324 Å in **8c**) regardless of the linker. Changing the methylene linker into a 2-methylbenzen-diyl linker shortened the Rh–P1 bonds in the diphosphene complexes (2.294 Å in **7'** *vs.* 2.310 Å in **10**), whereas the oppo-

Table 1 Selected structural parameters of rhodium complexes with a bidentate ligand including a phosphineborane moiety

	Experimental value			Calculated value ^a				
	7	8c ^b	9c ^c	7	7'	10	11	8c
$d(\text{P1–P2})/\text{\AA}$	2.0414(11)	—	—	2.051	2.043	2.043	—	—
$d(\text{Rh–P1})/\text{\AA}$	2.2694(8)	2.2743(7)	2.2483(4)	2.345	2.294	2.310	2.390	2.324
WBI (Rh–P1) ^d	—	—	—	0.509	0.558	0.551	0.501	0.532
$d(\text{Rh} \cdots \text{B})/\text{\AA}$	2.348(4)	2.313(3)	2.331(2)	2.394	2.392	2.404	2.375	2.375
$d(\text{P3–B})/\text{\AA}$	1.927(4)	1.923(3)	1.928(3)	1.929	1.932	1.939	1.919	1.939
$\text{deg}(\text{P1–Rh–B})/^\circ$	92.97(9)	87.26(8)	87.35(4)	93.9	92.3	84.6	96.1	86.9

^a Calculated at M06/SDD (Rh) and 6-31G(d) (other atoms) level of theory. ^b Ref. 27a. ^c Ref. 27b. ^d Wiberg bond index of the Rh–P1 bond.



site trend was observed in the phosphine complexes (2.390 Å in **11** vs. 2.324 Å in **8c**). Although the reason for the difference is unclear at present, the rhodium complex with a 2-methylbenzen-diyl linker may be strongly affected by the steric effect of the substituents on the phosphorus atom. In fact, phosphine complex **11** with a 2-methylbenzen-diyl linker has the longest Rh–P1 bond (2.390 Å) that markedly differed from the others. The Wiberg bond index of the Rh–P1 bond ranges from 0.501 to 0.558, indicating comparable Rh–P bond strengths between the diphosphenes and the phosphines. On the other hand, the different bonding character of the P1 atom in the diphosphenes (two coordinate) and the phosphines (three coordinate) affected the Rh–P bond properties. NBO analysis showed the localized lone-pair character of P1 (1.60e, $sp^{0.34}$) in **7** and the Rh–P1 bond character (1.95e, $sd^{7.33}$ for Rh and $sp^{2.04}$ for P) in **8c**.

The photophysical properties of **7** were evaluated from the UV-vis spectrum measured in CH_2Cl_2 solution. The UV-vis spectrum showed featureless and broad band tailing to 570 nm with a shoulder at 398 nm (Fig. 3a). TD-DFT calculations of **7** at TD-M06/SDD (Rh) and 6-311+G(2d,p) (other atoms) level of theory showed 10 transitions larger than 350 nm with a small oscillator strength ($f = 0.0033$ –0.0649, Table S8†) including the HOMO–LUMO transition at 497.5 nm ($f = 0.0084$). The HOMO is the lone-pair n_+ orbital of the P=P bond and the d orbital of rhodium, whereas the LUMO is the dominant contribution of the π^* orbital of the P=P bond (Fig. 3b). The character of the low-lying LUMO of the P=P bond was maintained even in **7**. The π orbital of the P=P bond was found in HOMO–2 together with the contribution of the d orbital of rhodium and the π orbital of the benzene ring of the Mes* group.

Investigation of catalytic properties of diphosphene–rhodium complex **7**

We investigated the catalytic properties of newly obtained diphosphene–rhodium complex **7**. To our regret, complex **7** did not act as an active catalyst in the hydroboration of vinylarene with catecholborane^{27c} or the intramolecular hydroamination of 5-(*N*-benzylamino)pentene.³¹ Nevertheless, after investigating several reactions, we found that complex **7** promoted the coupling reaction of benzimidazole (**12**) with cyclohexylallene (**13**) although the yield was low (Table 2):³² mixing **12** and 5 equiv. of **13** in the presence of 2.5 mol% of complex **7** in 1,2-dichloroethane (DCE) at 80 °C for 24 h afforded coupling product **14** in 35% yield (entry 1). The yield was decreased to 17% and 0% when the temperature was lowered to 70 °C and 60 °C, respectively (entries 2 and 3). No product **14** was obtained when $[\text{Rh}(\text{cod})_2]\text{BF}_4$ was used instead of **7** (entry 4). We confirmed that a new phosphorus species was generated by the reaction of **7** with **12** (7.5 equiv.) in DCE as judged from the ^{31}P NMR spectrum measured at room temperature. On the other hand, complex **7** was stable at room temperature in the presence of **13** (10 equiv.) but was converted into a new species at 80 °C. None of these new products could be characterized. Because the ligand exchange reaction with the diphosphene

Table 2 Coupling reaction of benzimidazole (**12**) with cyclohexylallene (**13**)

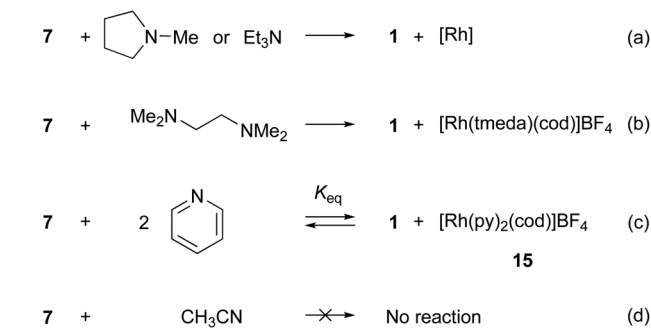
Entry	Rh complex	T (°C)	Yield ^a (%)
1	7	80	35
2	7	70	17
3	7	60	0
4	$[\text{Rh}(\text{cod})_2]\text{BF}_4$	80	0

^a Isolated yield.

ligand in **7** proceeded smoothly (*vide infra*), other phosphorus species generated from diphosphene–phosphineborane ligand **1** under the reaction conditions were likely the true active ligand.

Reaction of **7** with N-donor reagents

The fact that diphosphene–rhodium complex **7** easily reacts with benzimidazole (**12**) implies that other nitrogen-containing compounds should also be active reagents for **7**. If the phosphineborane moiety in **7** is converted into a phosphine, an electronically different diphosphene–rhodium complex with more robust coordination could be obtained. Thus, we investigated the deboration reaction of **7**. Treating *N*-methylpyrrolidine (20 equiv.) with a CD_2Cl_2 solution of **7** in an NMR tube and allowing the reaction mixture to stand for 4 h gave diphosphene–phosphineborane ligand **1** in a quantitative yield (Scheme 3a, Fig. S37†). The quantitative dissociation of **1** was also observed in the reaction with triethylamine (20 equiv.). The reaction took a longer time than that with *N*-methylpyrrolidine (approximately 2 days, Fig. S38†). In both reactions, the generated rhodium species could not be sufficiently characterized because rhodium complexes bearing



Scheme 3 Reactions of diphosphene–rhodium complex **7** with N-donor reagents. (tmeda = *N,N,N,N*-tetramethylethylenediamine, cod = 1,5-cyclooctadiene, py = pyridine); $K_{\text{eq}} = ([1][15])/([7][\text{py}]^2)$.



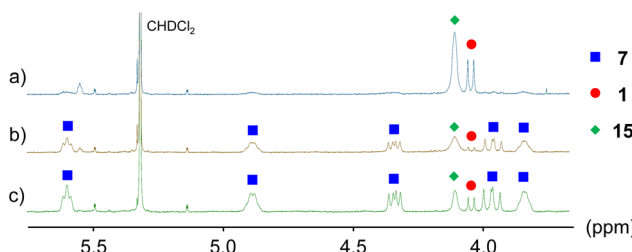


Fig. 4 ^1H NMR spectra measured in CD_2Cl_2 (a) after the reaction of **7** with pyridine (20 equiv.); (b) after removal of unreacted pyridine from the reaction mixture; and (c) after the treatment of **1** with $[\text{Rh}(\text{py})_2(\text{cod})]\text{BF}_4$ (**15**, 1 equiv.).

these tertiary amines and cod were not reported.³³ Although the reaction mechanism is unclear at present, the ligand exchange reaction between **1** and amines should be promoted by the high electron-accepting character of diphosphene because the LUMO is the dominant contribution of the π^* orbital of the $\text{P}=\text{P}$ bond (Fig. 3b). To characterize the rhodium species after the ligand exchange reaction, *N,N,N,N*-tetramethylethylenediamine (tmeda) was used. The reaction of **7** with tmeda (20 equiv.) in CD_2Cl_2 resulted in the formation of a 1 : 1 mixture of diphosphene–phosphineborane ligand **1** and $[\text{Rh}(\text{tmeda})(\text{cod})]\text{BF}_4$ (Scheme 3b, Fig. S39†) as judged from the ^1H NMR spectrum.³⁴ The result clearly showed that the dissociation of diphosphene–phosphineborane ligand **1** was faster than that of cod. The facile dissociation of **1** with tertiary amines prompted us to evaluate the coordination ability of diphosphene–phosphineborane ligand **1** toward rhodium. As a result, we found that the reaction of diphosphene–rhodium complex **7** with pyridine (py) gave an equilibrium mixture of **7**, pyridine, diphosphene–phosphineborane ligand **1**, and $[\text{Rh}(\text{py})_2(\text{cod})]\text{BF}_4$ (**15**; Scheme 3c, Fig. 4a).³⁴ Starting diphosphene–rhodium complex **7** was recovered after removal of unreacted pyridine under reduced pressure from a mixture of **7** and pyridine (20 equiv.) in CD_2Cl_2 solution, and its ^1H NMR spectrum was measured in CD_2Cl_2 (Fig. 4b). Treatment of **1** with **15** also afforded a mixture of **1**, **15**, **7**, and pyridine (Fig. 4c). The equilibrium constant ($K_{\text{eq}} = ([\mathbf{1}][\mathbf{15}])/([\mathbf{7}][\text{py}]^2)$) was estimated to be 1.0(2) $\text{mol}^{-1} \text{L}^{-1}$ by pyridine titration of a CD_2Cl_2 solution of **7** (Table S1†). Thus, the coordination ability of **1** is comparable to that of pyridine even though **1** exhibits bidentate coordination. The weak coordination ability of the $\text{P}=\text{P}$ bond (instability of the obtained rhodium complex) impedes the formation of a stable rhodium complex with a monodentate diphosphene ligand by the ligand exchange reaction. Meanwhile, no ligand exchange occurred in the reaction with acetonitrile (Scheme 3d, Fig. S41†).

Conclusions

Diphosphene **1** with a phosphineborane tether was synthesized without affecting the phosphineborane to form a $\text{P}=\text{P}$ bond. Diphosphene–rhodium complex **7** was isolated

with the aid of the phosphineborane moiety. X-ray crystallographic analysis and NMR spectroscopy of **7** revealed a bidentate *cis*-coordination through the $\text{P}=\text{P}$ bond in an η^1 fashion and the BH_3 moiety in an η^2 fashion. Complex **7** catalyzed the coupling reaction of benzimidazole with cyclohexylallene although the reactive $\text{P}=\text{P}$ bond was likely converted into another phosphorus species under the reaction conditions. Theoretical calculations showed the dominant contribution of the π^* orbital of the $\text{P}=\text{P}$ bond even in complex **7**, and its high electron-accepting character should promote facile ligand exchange reaction with N-donor reagents despite the bidentate coordination of **1**. In particular, the reaction of diphosphene–rhodium complex **7** with pyridine gave an equilibrium mixture of **7**, pyridine, diphosphene–phosphineborane ligand **1**, and $[\text{Rh}(\text{py})_2(\text{cod})]\text{BF}_4$ (**15**) owing to the weak coordination ability of **1** toward rhodium. Although further improvements in the fascinating catalytic activity of the diphosphene–transition metal complexes are required, our fundamental studies on bidentate diphosphene–rhodium complex **7** are expected to contribute to catalytic chemistry in the near future. We are actively investigating the coordination behavior toward other transition metals and developing other types of multidentate ligands with the $\text{P}=\text{P}$ bond for use in catalytic organic transformations.

Author contributions

A. T.: Conceptualization, data curation, formal analysis, funding acquisition, investigation, project administration, validation, visualization, writing – original draft, writing – review and editing. S. T.: Data curation, formal analysis, investigation, visualization. K. K.: Funding acquisition, supervision, writing – review and editing.

Conflicts of interest

There are no conflicts to declare.

Acknowledgements

This work was supported by Grants-in-Aid for Scientific Research (B: #22H02081 and #22K19035 to K. K.; and C: #21K05071 to A. T.) from the JSPS (Japan). The authors thank Professor Ikuko Miyahara (Osaka Metropolitan University) for assistance in X-ray crystallographic analysis; Professor Hajime Kameo (Osaka Metropolitan University) for assistance in the measurement of IR spectra; and Professor Hideki Fujiwara and Professor Daisuke Sakamaki (Osaka Metropolitan University) for allowing access to the UV-vis spectrophotometer. All theoretical calculations were carried out at the Research Centre (21-IMS-C029) for Computational Science (Japan).



References

1 (a) *Organophosphorus Chemistry: From Molecules to Applications*, ed. V. Iaroshenko, Wiley-VCH, 2019; (b) *Phosphorus: Chemistry, Biochemistry and Technology 6th*, ed. D. E. C. Corbridge, CRC Press Taylor & Francis Group, 2013; (c) *Phosphorus(iii) Ligands in Homogenous Catalysis: Design and Synthesis*, ed. P. C. J. Kamer and P. W. N. M. van Leeuwen, Wiley, 2012; (d) *Phosphorus Ligands in Asymmetric Catalysis*, ed. A. Börner, Wiley-VCH, 2008.

2 (a) F. Mathey, *Angew. Chem., Int. Ed.*, 2003, **42**, 1578–1604; (b) P. Le Floch, *Coord. Chem. Rev.*, 2006, **250**, 627–681; (c) C. Müller, L. E. E. Broeckx, I. de Krom and J. J. M. Weemers, *Eur. J. Inorg. Chem.*, 2013, 187–202; (d) F. Ozawa and Y. Nakajima, *Chem. Rec.*, 2016, **16**, 2314–2323; (e) N. T. Coles, A. S. Abels, J. Leitl, R. Wolf, H. Grützmacher and C. Müller, *Coord. Chem. Rev.*, 2021, **433**, 213729; (f) A. Ziolkowska, J. Doroszuk and Ł. Ponikiewski, *Organometallics*, 2023, **42**, 505–537.

3 Selected examples of phosphaalkene complexes: (a) W. Keim, R. Appel, S. Gruppe and F. Knoch, *Angew. Chem., Int. Ed. Engl.*, 1987, **26**, 1012–1013; (b) T. Minami, H. Okamoto, S. Ikeda, R. Tanaka, F. Ozawa and M. Yoshifuji, *Angew. Chem., Int. Ed.*, 2001, **40**, 4501–4503; (c) F. Ozawa, H. Okamoto, S. Kawagishi, S. Yamamoto, T. Minami and M. Yoshifuji, *J. Am. Chem. Soc.*, 2002, **124**, 10968–10969; (d) A. Ionkin and W. Marshall, *Chem. Commun.*, 2003, 710–711; (e) M. Freytag, S. Ito and M. Yoshifuji, *Chem. – Asian J.*, 2006, **1**, 693–700; (f) J. Dugal-Tessier, G. R. Dake and D. P. Gates, *Org. Lett.*, 2010, **12**, 4667–4669; (g) Y.-H. Chang, Y. Nakajima and F. Ozawa, *Organometallics*, 2013, **32**, 2210–2215; (h) K. Takeuchi, Y. Tanaka, I. Tanigawa, F. Ozawa and J.-C. Choi, *Dalton Trans.*, 2020, **49**, 3630–3637.

4 Selected examples of phosphinine complexes: (a) B. Breit, *Chem. Commun.*, 1996, 2071–2072; (b) B. Breit, R. Winde, T. Mackewitz, R. Paciello and K. Harms, *Chem. – Eur. J.*, 2001, **7**, 3106–3121; (c) M. T. Reetz and X. Li, *Angew. Chem., Int. Ed.*, 2005, **44**, 2962–2964; (d) J. J. M. Weemers, W. N. P. van der Graaff, E. A. Pidko, M. Lutz and C. Müller, *Chem. – Eur. J.*, 2013, **19**, 8991–9004; (e) R. J. Newland, M. F. Wyatt, R. L. Wingad and S. M. Mansell, *Dalton Trans.*, 2017, **46**, 6172–6176; (f) R. J. Newland, J. M. Lynam and S. M. Mansell, *Chem. Commun.*, 2018, **54**, 5482–5485; (g) M. Rigo, E. R. M. Habraken, K. Bhattacharyya, M. Weber, A. W. Ehlers, N. Mézailles, J. C. Slootweg and C. Müller, *Chem. – Eur. J.*, 2019, **25**, 8769–8779; (h) E. C. Trodden, M. P. Delve, C. Luz, R. J. Newland, J. M. Andresen and S. M. Mansell, *Dalton Trans.*, 2021, **50**, 13407–13411.

5 (a) L. Weber, *Chem. Rev.*, 1992, **92**, 1839–1906; (b) T. Sasamori and N. Tokitoh, *Dalton Trans.*, 2008, 1395–1408; (c) M. C. Simpson and J. D. Protasiewicz, *Pure Appl. Chem.*, 2013, **85**, 801–815; (d) M. Yoshifuji, *Eur. J. Inorg. Chem.*, 2016, 607–615; (e) L. Weber, F. Ebeler and R. S. Ghadwal, *Coord. Chem. Rev.*, 2022, **461**, 214499.

6 M. Yoshifuji, I. Shima, N. Inamoto, K. Hirotsu and T. Higuchi, *J. Am. Chem. Soc.*, 1981, **103**, 4587–4589.

7 (a) A. H. Cowley, A. Decken, N. C. Norman, C. Krüger, F. Lutz, H. Jacobsen and T. Ziegler, *J. Am. Chem. Soc.*, 1997, **119**, 3389–3390; (b) C. Dutan, S. Shah, R. C. Smith, S. Choua, T. Berclaz, M. Geoffroy and J. D. Protasiewicz, *Inorg. Chem.*, 2003, **42**, 6241–6251; (c) T. Sasamori, E. Mieda, N. Nagahora, K. Sato, D. Shiomi, T. Takui, Y. Hosoi, Y. Furukawa, N. Takagi, S. Nagase and N. Tokitoh, *J. Am. Chem. Soc.*, 2006, **128**, 12582–12588; (d) B. Lu, L. Wang, X. Jiang, G. Rauhut and X. Zeng, *Angew. Chem., Int. Ed.*, 2023, **62**, e202217353.

8 A. Tsurusaki, R. Ura and K. Kamikawa, *Organometallics*, 2020, **39**, 87–92.

9 (a) J. C. Green, M. L. H. Green and G. E. Morris, *J. Chem. Soc., Chem. Commun.*, 1974, 212–213; (b) P. S. Elmes, M. L. Scudder and B. O. West, *J. Organomet. Chem.*, 1976, **122**, 281–288.

10 For recent investigations on diphosphene complexes: (a) C. Taube, J. Fidelius, K. Schwedtmann, C. Ziegler, F. Kreuter, L. Loots, L. J. Barbour, R. Tonner-Zech, R. Wolf and J. J. Weigand, *Angew. Chem., Int. Ed.*, 2023, **62**, e202306706; (b) A. Schmer, D. Welideniya, T. Terschüren, G. Schnakenburg, J. Daniels, A. Bauza, A. Frontera and R. Streubel, *Dalton Trans.*, 2021, **50**, 17892–17896; (c) A. Schmer, A. Bauza, G. Schnakenburg, A. Frontera and R. Streubel, *Dalton Trans.*, 2021, **50**, 2131–2137; (d) D. Dhara, D. Scheschkewitz, V. Chandrasekhar, C. B. Yildiz and A. Jana, *Chem. Commun.*, 2021, **57**, 809–812.

11 N. Nagahora, T. Sasamori, Y. Watanabe, Y. Furukawa and N. Tokitoh, *Bull. Chem. Soc. Jpn.*, 2007, **80**, 1884–1900.

12 (a) B. A. Surgenor, M. Bühl, A. M. Z. Slawin, J. D. Woollins and P. Kilian, *Angew. Chem., Int. Ed.*, 2012, **51**, 10150–10153; (b) B. A. Surgenor, B. A. Chalmers, K. S. A. Arachchige, A. M. Z. Slawin, J. D. Woollins, M. Bühl and P. Kilian, *Inorg. Chem.*, 2014, **53**, 6856–6866.

13 S. C. Kosnik, J. F. Binder, M. C. Nascimento, A. Swidan and C. L. B. Macdonald, *Chem. – Eur. J.*, 2019, **25**, 1208–1211.

14 (a) P. Barbaro, A. Ienco, C. Mealli, M. Peruzzini, O. J. Scherer, G. Schmitt, F. Vizza and G. Wolmershäuser, *Chem. – Eur. J.*, 2003, **9**, 5195–5210; (b) P. Barbaro, M. Caporali, A. Ienco, C. Mealli, M. Peruzzini and F. Vizza, *Eur. J. Inorg. Chem.*, 2008, 1392–1399.

15 R. Ura, A. Tsurusaki and K. Kamikawa, *Dalton Trans.*, 2022, **51**, 2943–2952.

16 Examples of rhodium complexes of phosphaalkenes: (a) R. S. Jensen, K. Umeda, M. Okazaki, F. Ozawa and M. Yoshifuji, *J. Organomet. Chem.*, 2007, **692**, 286–294; (b) A. Hayashi, M. Okazaki and F. Ozawa, *Organometallics*, 2007, **26**, 5246–5249; (c) T. Matsumoto, T. Sasamori, H. Miyake and N. Tokitoh, *Organometallics*, 2014, **33**, 1341–1344; (d) P. M. Miura-Akagi, M. L. Nakashige, C. K. Maile, S. M. Oshiro, J. R. Gurr, W. Y. Yoshida, A. T. Royappa, C. E. Krause, A. L. Rheingold, R. P. Hughes and M. F. Cain, *Organometallics*, 2016, **35**, 2224–2231; (e) P. Gupta,



T. Taeufer, J.-E. Siewert, F. Reiß, H.-J. Drexler, J. Pospech, T. Beweries and C. Hering-Junghans, *Inorg. Chem.*, 2022, **61**, 11639–11650.

17 Examples of rhodium complexes of phosphinines: (a) B. Schmid, L. M. Venanzi, T. Gerfin, V. Gramlich and F. Mathey, *Inorg. Chem.*, 1992, **31**, 5117–5122; (b) X. Sava, N. Mézailles, N. Maigrot, F. Nief, L. Ricard, F. Mathey and P. Le Floch, *Organometallics*, 1999, **18**, 4205–4215; (c) A. C. Carrasco, E. A. Pidko, A. M. Masdeu-Bultó, M. Lutz, A. L. Spek, D. Vogt and C. Müller, *New J. Chem.*, 2010, **34**, 1547–1550; (d) L. E. E. Broeckx, M. Lutz, D. Vogt and C. Müller, *Chem. Commun.*, 2011, **47**, 2003–2005; (e) X. Chen, Z. Li and H. Grützmacher, *Chem. – Eur. J.*, 2018, **24**, 8432–8437; (f) R. J. Newland, J. M. Lynam and S. M. Mansell, *Chem. Commun.*, 2018, **54**, 5482–5485; (g) K. Masada, S. Kusumoto and K. Nozaki, *Angew. Chem. Int. Ed.*, 2022, **61**, e202117096.

18 T. Fanjul, G. Eastham, J. Floure, S. J. K. Forrest, M. F. Haddow, A. Hamilton, P. G. Pringle, A. G. Orpen and M. Waugh, *Dalton Trans.*, 2013, **42**, 100–115.

19 (a) K. Kamijo, A. Otoguro, K. Toyota and M. Yoshifuji, *Bull. Chem. Soc. Jpn.*, 1999, **72**, 1335–1342; (b) S. Kawasaki, T. Fujita, K. Toyota and M. Yoshifuji, *Bull. Chem. Soc. Jpn.*, 2005, **78**, 1082–1090.

20 Y. Ma, F. Chen, J. Bao, H. Wei, M. Shi and F. Wang, *Tetrahedron Lett.*, 2016, **57**, 2465–2467.

21 G. Müller, H.-P. Abicht, M. Waldkircher, J. Lachmann, M. Lutz and M. Winkler, *J. Organomet. Chem.*, 2001, **622**, 121–134.

22 For an example of the introduction of a phosphine moiety after the halogen/lithium exchange from a compound with a borane-protected phosphinomethyl group: Q. Shen, T. Ogata and J. F. Hartwig, *J. Am. Chem. Soc.*, 2008, **130**, 6586–6596.

23 (a) G. C. Lloyd-Jones and N. P. Taylor, *Chem. – Eur. J.*, 2015, **21**, 5423–5428; (b) A. Zhdanko, B. A. van der Worp and S. Lemaire, *Eur. J. Org. Chem.*, 2022, e202200130.

24 (a) M. Yoshifuji, K. Shibayama, N. Inamoto, T. Matsushita and K. Nishimoto, *J. Am. Chem. Soc.*, 1983, **105**, 2495–2497; (b) A. Tsurusaki, R. Ura and K. Kamikawa, *Dalton Trans.*, 2018, **47**, 4437–4441.

25 L. Routaboul, F. Toulgoat, J. Gatignol, J.-F. Lohier, B. Norah, O. Delacroix, C. Alayrac, M. Taillefer and A.-C. Gaumont, *Chem. – Eur. J.*, 2013, **19**, 8760–8764.

26 (a) K. Miqueu, J.-M. Sotiropoulos, G. Pfister-Guillouzo, H. Ranaivonjatovo and J. Escudié, *J. Mol. Struct.*, 2001, **545**, 139–146; (b) T. Sasamori, N. Takeda and N. Tokitoh, *J. Phys. Org. Chem.*, 2003, **16**, 450–462; (c) Y. Amatatsu, *J. Phys. Chem. A*, 2008, **112**, 8824–8828; (d) H.-L. Peng, J. L. Payton, J. D. Protasiewicz and M. C. Simpson, *J. Phys. Chem. A*, 2009, **113**, 7054–7063. See also references cited therein.

27 (a) M. Ingleson, N. J. Patmore, G. D. Ruggiero, C. G. Frost, M. F. Mahon, M. C. Willis and A. S. Weller, *Organometallics*, 2001, **20**, 4434–4436; (b) D. H. Nguyen, H. Lauréano, S. Jugé, P. Kalck, J.-C. Daran, Y. Coppel, M. Urrutigoity and M. Gouygou, *Organometallics*, 2009, **28**, 6288–6292; (c) D. H. Nguyen, J. Bayardon, C. Salomon-Bertrand, S. Jugé, P. Kalck, J.-C. Daran, M. Urrutigoity and M. Gouygou, *Organometallics*, 2012, **31**, 857–869; (d) C. Salomon-Bertrand, J. Bayardon, H. Lauréano, S. Jugé, J.-C. Daran and M. Gouygou, *J. Organomet. Chem.*, 2021, **938**, 121753.

28 A. M. Trzeciak and J. J. Ziolkowski, *J. Organomet. Chem.*, 1992, **429**, 239–244.

29 M. K. Kesharwani, B. Brauer and J. M. L. Martin, *J. Phys. Chem. A*, 2015, **119**, 1701–1714.

30 (a) D. V. Partyka, M. P. Washington, T. G. Gray, J. B. Updegraff III, J. F. Turner II and J. D. Protasiewicz, *J. Am. Chem. Soc.*, 2009, **131**, 10041–10048; (b) X. Pan, L. Zhang, Y. Zhao, G. Tan, H. Ruan and X. Wang, *Chin. J. Chem.*, 2020, **38**, 351–355; (c) S. Lauk, M. Zimmer, B. Morgenstern, V. Huch, C. Müller, H. Sitzmann and A. Schäfer, *Organometallics*, 2021, **40**, 618–626.

31 Z. Liu and J. F. Hartwig, *J. Am. Chem. Soc.*, 2008, **130**, 1570–1571.

32 K. Xu, N. Thieme and B. Breit, *Angew. Chem., Int. Ed.*, 2014, **53**, 2162–2165.

33 The reaction of $[\text{Rh}(\text{cod})_2]\text{BF}_4$ with *N*-methylpyrrolidine or triethylamine gave a complex mixture.

34 $[\text{Rh}(\text{tmida})(\text{cod})]\text{BF}_4$ and $[\text{Rh}(\text{py})_2(\text{cod})]\text{BF}_4$ (**15**) were synthesized by the reaction of $[\text{Rh}(\text{cod})_2]\text{BF}_4$ with tmida and pyridine, respectively (see ESI).†

